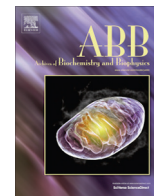




Contents lists available at ScienceDirect

## Archives of Biochemistry and Biophysics

journal homepage: [www.elsevier.com/locate/yabbi](http://www.elsevier.com/locate/yabbi)

## Exploration of the six tryptophan residues of *Escherichia coli* cystathionine $\beta$ -lyase as probes of enzyme conformational change



Allison F. Jaworski, Susan M. Aitken\*

Department of Biology, Carleton University, Ottawa K1S 5B6, Canada

## ARTICLE INFO

## Article history:

Received 13 May 2013  
and in revised form 6 July 2013  
Available online 19 August 2013

## Keywords:

Pyridoxal 5'-phosphate  
Tryptophan fluorescence  
Site-directed mutagenesis  
Amino acid metabolism  
Cystathionine

## ABSTRACT

Cystathionine  $\beta$ -lyase (CBL) catalyzes the hydrolysis of L-cystathionine (L-Cth), producing L-homocysteine (L-Hcys), pyruvate and ammonia, in the second step of the transsulfuration pathway of bacteria and plants. A series of 17 site-directed variants of *Escherichia coli* CBL (eCBL) was constructed to probe the contributions of the six tryptophan residues (W131, W188, W230, W276, W300 and W340) to the fluorescence spectrum of eCBL and to assess their mutability and utility as conformational probes. The effects of these Trp  $\rightarrow$  Phe substitutions on  $k_{cat}$  and  $K_m^{L-Cth}$  are less than 2-fold, with the exception of the 8-fold increase in  $K_m^{L-Cth}$  observed for eCBL-W340F. The midpoint of thermal denaturation, as monitored by circular dichroism spectroscopy, is reduced 4.7 °C by the W188F substitution while the targeted replacement of the other five tryptophans alter  $T_m$  by less than 1.7 °C. The fluorescence spectrum of eCBL is dominated by W230 and the contribution of W340, situated in the active site, is minor. The observed 5-fold increase in the 336 nm fluorescence emission of W188 between 0 and 2 M urea, suggests a conformational change at the domain interface. Residues W188 and W340, conserved in proteobacterial CBL enzymes, are situated at the core of the domain interface that forms the active-site cleft. The results of this study suggest that W188 is a useful probe of subtle conformational changes at the domain interface and active site.

© 2013 Elsevier Inc. All rights reserved.

## Introduction

Cystathionine  $\beta$ -lyase (CBL)<sup>1</sup> follows cystathionine  $\gamma$ -synthase (CGS) in the bacterial transsulfuration pathway. These two closely related enzymes catalyze the pyridoxal 5'-phosphate (PLP)-dependent formation of L-cystathionine (L-Cth), via the condensation of O-succinyl-L-homoserine (OSHS) and L-cysteine (L-Cys), and its subsequent hydrolysis, producing pyruvate, ammonia and L-homocysteine (L-Hcys), the immediate precursor of L-methionine [1–4]. The enzymes of the bacterial transsulfuration pathway are attractive targets for the development of novel anti-microbial compounds

because they are not present in mammals, which derive L-Cys from L-Hcys via the reverse transsulfuration pathway. There are structures available for 20 members of the  $\gamma$ -subfamily within the large and catalytically diverse fold-type I classification of PLP-dependent enzymes. These represent seven distinct enzymes from diverse species: CBL, CGS, cystathionine  $\gamma$ -lyase (CGL) – the second enzyme of the reverse transsulfuration pathway, methionine  $\gamma$ -lyase (MGL), homocysteine  $\gamma$ -lyase, O-acetylhomoserine sulfhydrylase and O-succinylhomoserine sulfhydrylase [5]. Comparison of these enzymes reveals conservation of overall structure as well as active-site features and residues [2,3,6]. Recent studies probing the active-sites of *Escherichia coli* CBL (eCBL) and CGS (eCGS) for determinants of substrate and reaction specificity have reported that the roles of conserved residues are dependent on the context of the specific enzyme [5,7,8]. This illustrates the subtlety of the mechanisms underlying specificity and demonstrates the need to explore structure–function relationships, including the subtle differences in active-site architecture and dynamics and the positioning of key residues, to enable the design of selective inhibitors as well as engineering of the enzymes within this family.

The eCBL monomer is comprised of three domains, which each possess active-site residues. Residues 1–60 form the amino-terminal domain that contributes to the active-site of the neighboring monomer. The catalytic (residues 61–256) and carboxy-terminal

\* Corresponding author. Fax: +1 (613) 520 3539.

E-mail address: [susan\\_aitken@carleton.ca](mailto:susan_aitken@carleton.ca) (S.M. Aitken).

<sup>1</sup> Abbreviations used: AAT, aspartate aminotransferase; CBL, cystathionine  $\beta$ -lyase; eCBL, *Escherichia coli* CBL; CGL, cystathionine  $\gamma$ -lyase; CGS, cystathionine  $\gamma$ -synthase; eCGS, *E. coli* CGS; L-Cth, L-cystathionine; DTNB, 5,5'-dithiobis(2-nitrobenzoic acid); FRET, fluorescence resonance energy transfer; L-Hcys, L-homocysteine; MGL, methionine  $\gamma$ -lyase; Ni-NTA, Ni-nitrilo triacetic acid; L-OSHS, O-succinyl-L-homoserine; PLP, pyridoxal 5'-phosphate; sOASS, *Salmonella typhimurium* O-acetylserine sulfhydrylase. eCBL Trp  $\rightarrow$  Phe variants (defined individually in Table 1) are identified as follows: individual Trp  $\rightarrow$  Phe substitutions: W131F, W188F, W230F, W276F, W300F, W340F; triple substitution variant (tX): W131F + W230F + W276F; pentuple substitution variants (pX) are identified by the remaining tryptophan residue, e.g. pXW131 = W188F + W230F + W276F + W300F + W340F; all tryptophan residues of the hextuple variant (hX) are replaced: W131F + W188F + W230F + W276F + W300F + W340F.

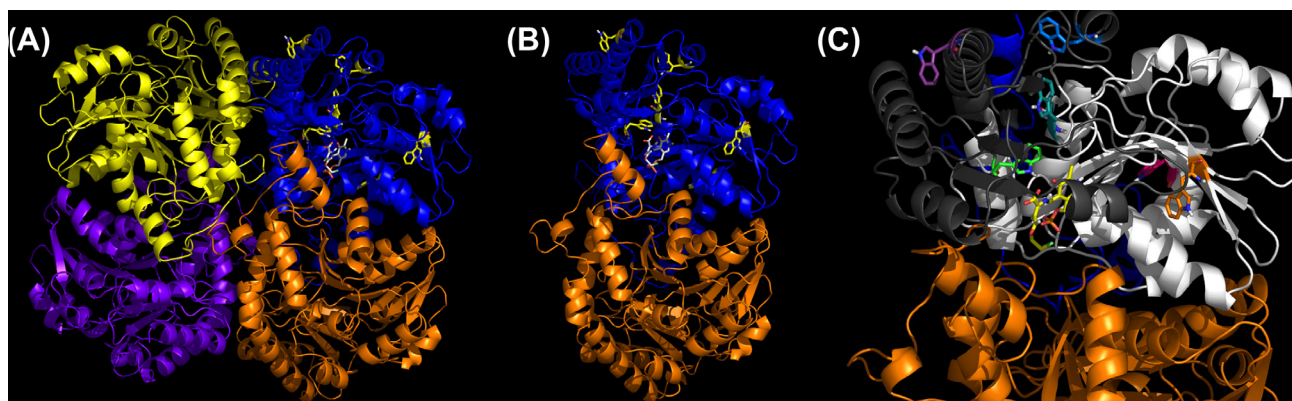


**Fig. 1.** The location of the six tryptophan residues (yellow) of eCBL in the context of the (A) homotetramer and (B) catalytic dimer. (C) The active site, containing the PLP cofactor (yellow) is situated at the interface between the catalytic (residues 61–256, white) and carboxy-terminal (residues 257–395, grey) domains. The amino-terminal domain (residues 1–60, dark blue) contributes to the active site of the neighboring subunit. Tryptophan residues are highlighted to illustrate their relative positions: W131 (orange), W188 (teal), W230 (pink), W276 (purple), W300 (blue) and W340 (green). (For interpretation of the references to colour in this figure legend, the reader is referred to the web version of this article.)

(residues 257–395) domains form the two sides of the active-site cleft (Fig. 1) [2]. The central location of W188 and W340 within the active-site cleft provides potential probe(s) of changes in active-site conformation, either during catalysis or resulting from protein engineering studies. A series of 17 site-directed variants of eCBL residues W131, W188, W230, W276, W300 and W340 was constructed and characterized to determine the efficacy of native tryptophan residues as conformational probes.

## Materials and methods

### Reagents

L-Cth was purchased from Sigma. Ni-nitrilotriacetic acid (Ni-NTA) resin and 5,5'-dithiobis(2-nitrobenzoic acid) (DTNB) were obtained from Qiagen and Pierce, respectively. Oligonucleotide primers were synthesized by Integrated DNA Technologies and site-directed mutants were sequenced by BioBasic prior to expression and purification to ensure only the desired mutation(s) were present for each Trp → Phe variant.

### Construction, expression and purification of site-directed variants

Site-directed variants of eCBL, constructed via the overlap-extension polymerase chain reaction method, were inserted into the pTrc-99aAF plasmid [9]. Wild-type and site-directed variants of eCBL were expressed in the *E. coli* ER1821 *metC::cat* strain, in which the gene encoding eCBL is replaced by *cat*, encoding resistance to chloramphenicol, to prevent contamination with the wild-type *E. coli* enzyme [9]. The eCBL enzymes were expressed and purified, via Ni-NTA affinity chromatography, as described by Farsi et al. [9]

### Determination of steady-state kinetic parameters

Enzyme activity was measured in a total volume of 100  $\mu$ L at 25  $^{\circ}$ C on a Spectramax 340 microtiter plate spectrophotometer (Molecular Devices). The assay buffer was comprised of 50 mM Tris, pH 8.5, with 20  $\mu$ M PLP. The hydrolysis of L-Cth was detected using 2 mM DTNB ( $\epsilon_{412} = 13,600 \text{ M}^{-1}\text{s}^{-1}$ ), which reacts with the sulfhydryl group of the L-Hcys product [10]. A background reading was recorded before initiating the reaction with the eCBL enzyme. Values of  $k_{\text{cat}}^{\text{L-Cth}}$  and  $K_{\text{m}}^{\text{L-Cth}}$  were obtained by fitting of the data to

the Michaelis–Menten equation and  $k_{\text{cat}}^{\text{L-Cth}}/K_{\text{m}}^{\text{L-Cth}}$  was obtained independently from Eq. 1.

$$\frac{v}{[E]} = \frac{k_{\text{cat}}/K_{\text{m}}^{\text{L-Cth}} \times [L - \text{Cth}]}{1 + [L - \text{Cth}]/K_{\text{m}}^{\text{L-Cth}}} \quad (1)$$

### Fluorescence and far-UV circular dichroism spectra of eCBL

Fluorescence spectra of wild-type and variants of eCBL in 20 mM potassium phosphate, pH 7.5, were recorded with a Varian Cary Eclipse spectrophotometer in a 1 cm path-length cell at 25  $^{\circ}$ C, with 5 nm slits. Similarly, far-UV CD spectra of 5.6  $\mu$ M enzyme were recorded on a Jasco-J815 spectropolarimeter in a 1 mm path-length cell by averaging five scans from 260 to 200 nm (1 nm bandwidth) in 0.2 nm steps at a rate of 20 nm/min. The ellipticity at 222 nm (1 nm bandwidth) was measured between 20 and 80  $^{\circ}$ C with instrument parameters set to  $\Delta T$  of 18  $^{\circ}$ C/hr with a 1  $^{\circ}$ C step resolution.

### Urea denaturation of eCBL

Wild-type and tryptophan replacement variants of eCBL were incubated at 25  $^{\circ}$ C with 0–8 M urea for 26 h in 20 mM phosphate buffer, pH 7.5. Fluorescence spectra of 1  $\mu$ M wild-type eCBL and Trp → Phe variants and 5.6  $\mu$ M wild-type eCBL, and far-UV CD spectra of 5.6  $\mu$ M wild-type enzyme were recorded. To assess the ability of eCBL to refold following urea denaturation, 30  $\mu$ M wild-type eCBL was incubated in 1.4, 2.5, 3, 5 and 8 M urea. Enzyme from each treatment was subsequently diluted in 20 mM phosphate, pH 7.5, to a final enzyme concentration of 1  $\mu$ M, and incubated for a further 26 h at 25  $^{\circ}$ C prior to recording of fluorescence spectra and measurement of specific activity at 2.5 mM L-Cth.

## Results

Residues W188 and W340 are situated at the core and W131 and W300 are located at the periphery of the interface of the catalytic and carboxy-terminal domains, which forms the active-site cleft of eCBL (Fig. 1) [2]. These tryptophans provide potential probe(s) of inter-domain and/or active-site conformational changes. A set of 17 Trp → Phe replacement variants, targeting the six tryptophan residues of eCBL (W131, W188, W230, W276, W300 and W340), was constructed to characterize the contribution of each to the

fluorescence spectrum of eCBL and the effect of their substitution on activity and stability.

#### Effect of Trp → Phe substitution on the activity, stability and fluorescence spectrum of eCBL

The 17 site-directed variants of eCBL are soluble with yields of at least 7 mg/L. The yields of the Trp → Phe replacement variants targeting one, three or four, and five or six of the six tryptophan residues of eCBL were 35–68, 8–22 and 7–10 mg/L, respectively. This is similar to the 15–41 and 56 mg/L values reported for 15 single-substitution active-site variants of eCBL and the wild-type enzyme, respectively [5,7,9]. Replacement of W340 with phenylalanine precludes the formation of hydrogen bonds with the 3' hydroxyl moiety of PLP and the  $\alpha$ -carboxylate group of the substrate, bound in Schiff base linkage with the cofactor, and results in a 8-fold increase in  $K_{m}^{l-Cth}$  (Table 1) [2,7]. With the exception of those including the W340F substitution, all variants possess near-native levels of the physiological  $\alpha,\beta$ -elimination activity. The  $k_{cat}$  and  $K_{m}^{l-Cth}$  values of the W131F, W188F, W230F, W276F and W300F variants are within 1.6-fold of the wild-type enzyme (Table 1). The minor 3–30% and 2–45% changes in  $k_{cat}$  and  $k_{cat}/K_{m}^{l-Cth}$  of W131F, W188F, W230F, W276F and W300F are largely additive and, for example, account for the 42% and 54% decreases in these parameters, respectively, of the pXW340 variant, for which all tryptophans except W340 have been replaced by phenylalanine.

Loss of  $\alpha$ -helical structure, as determined by circular dichroism spectroscopy, was employed to assess the relative thermostability of each site-directed variant, compared to the wild-type enzyme. Substitution of W131, W230 or W300 results in increases in  $T_m$  of 1.2–1.7 °C. In contrast, W340F has no effect and W276F decreases  $T_m$  by 1.0 °C. The 4.7 °C decrease in  $T_m$  observed for W188F is unique among the single substitution variants and is evident in each of the multi-residue substitution variants containing the W188F substitution (Table 1, Fig. 2). For example, the  $T_m$  value of the tX (W131F, W230F, W276) variant is 5.6 °C higher than tX + W188F, and the latter is decreased 2.7 °C compared to the wild-type enzyme. The minor stabilizing effect of the other Trp → Phe substitutions is generally additive, as evidenced by the pXW188 variant in which all Trp residues, with the exception of W188, have been replaced with Phe, and hX, which contains all six Trp → Phe substitutions. The  $T_m$  values of the pXW188 and hX proteins, which differ only in the presence of W188 in the former, are 6.1 and 1.7 °C higher than the wild-type eCBL enzyme,

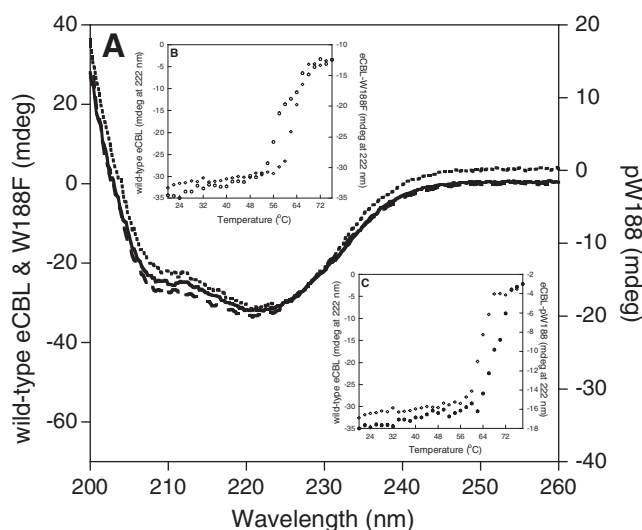


**Fig. 2.** Residue W188 possesses distinct properties compared to the other Trp residues of eCBL. The circular dichroism (A) spectra and (B and C) thermal denaturation profiles at 222 nm of 5.6  $\mu$ M wild-type (solid line, open diamond) and the single W188F (dashed line, open circle) and pentuple pXW188 (dotted line, closed circle) variants of eCBL.

respectively (Table 1, Figs. 2 and 3). The 4.4 °C difference between pXW188 and hX is similar to the 4.7 °C decrease in  $T_m$  of W188F compared to wild-type eCBL.

The far-UV circular dichroism spectrum of eCBL is not affected by substitution of any of the six tryptophan residues, as illustrated when comparing the spectra of wild-type eCBL and the W188F, pXW188 (Fig. 2A) and hX (Fig. 3B) variants. Comparison of the fluorescence spectra ( $\lambda_{ex} = 295$  nm) of the single and pentuple Trp → Phe substitution variants, replacing one and five of the six tryptophan residues of eCBL, respectively, demonstrates that while W230 dominates the fluorescence spectrum of eCBL, the contribution of W340 is minor (Fig. 4).

#### Urea denaturation of eCBL

The fluorescence profile for urea denaturation of eCBL is complex. The broad emission spectrum of eCBL is increased 5-fold in intensity at 336 nm between 0 and 2 M urea, with subsequent

**Table 1**  
 $T_m$  values and kinetic parameters of the  $\alpha,\beta$ -elimination of l-Cth for wild-type site-directed variants of eCBL.<sup>a</sup>

Enzyme	Trp remaining	$k_{cat}$ ( $s^{-1}$ )	$K_{m}^{l-Cth}$ (mM)	$k_{cat}/K_{m}^{l-Cth}$ ( $M^{-1}s^{-1}$ )	$T_m$ (°C)
eCBL	W131, W188, W230, W276, W300, W340	54.5 ± 0.7	0.116 ± 0.007	(4.7 ± 0.3) × 10 <sup>5</sup>	62.9 ± 0.2
W131F	W188, W230, W276, W300, W340	45.3 ± 0.7	0.101 ± 0.008	(4.5 ± 0.3) × 10 <sup>5</sup>	64.1 ± 0.2
W188F	W131, W230, W276, W300, W340	38.1 ± 0.2	0.121 ± 0.003	(3.15 ± 0.06) × 10 <sup>5</sup>	58.1 ± 0.4
W230F	W131, W188, W276, W300, W340	55.9 ± 0.7	0.19 ± 0.01	(3.0 ± 0.1) × 10 <sup>5</sup>	64.1 ± 0.2
W276F	W131, W188, W230, W300, W340	60.4 ± 0.6	0.131 ± 0.006	(4.6 ± 0.2) × 10 <sup>5</sup>	61.9 ± 0.2
W300F	W131, W188, W230, W276, W340	42.5 ± 0.4	0.161 ± 0.007	(2.6 ± 0.1) × 10 <sup>5</sup>	64.6 ± 0.3
W340F	W131, W188, W230, W276, W300	60.7 ± 0.5	0.91 ± 0.05	(6.6 ± 0.1) × 10 <sup>4</sup>	63.2 ± 0.3
tX (W131F/W230F/W276F)	W188, W300, W340	54.5 ± 0.4	0.171 ± 0.006	(3.2 ± 0.1) × 10 <sup>5</sup>	65.8 ± 0.2
tX + W188F	W300, W340	25.4 ± 0.9	0.27 ± 0.04	(9.4 ± 0.1) × 10 <sup>4</sup>	60.2 ± 0.3
tX + W300F	W188, W340	74 ± 1	0.31 ± 0.03	(2.4 ± 0.2) × 10 <sup>5</sup>	65.6 ± 0.2
tX + W340F	W188, W300	65 ± 3	1.0 ± 0.1	(6.6 ± 0.7) × 10 <sup>4</sup>	66.7 ± 0.3
pXW131	W131	42 ± 1	2.0 ± 0.1	(2.1 ± 0.1) × 10 <sup>4</sup>	62.6 ± 0.3
pXW188	W188	54 ± 1	1.26 ± 0.08	(4.3 ± 0.2) × 10 <sup>4</sup>	69.0 ± 0.7
pXW230	W230	35.1 ± 0.9	1.05 ± 0.09	(3.3 ± 0.2) × 10 <sup>4</sup>	63.4 ± 0.3
pXW276	W276	38 ± 2	2.1 ± 0.2	(1.8 ± 0.1) × 10 <sup>4</sup>	66.4 ± 0.6
pXW300	W300	40 ± 1	1.8 ± 0.1	(2.3 ± 0.1) × 10 <sup>4</sup>	64.6 ± 0.3
pXW340	W340	31.7 ± 0.3	0.148 ± 0.007	(2.13 ± 0.09) × 10 <sup>5</sup>	63.1 ± 0.4
hX (all W → F)	No Trp	46 ± 2	1.8 ± 0.2	(2.5 ± 0.1) × 10 <sup>4</sup>	64.6 ± 0.3

<sup>a</sup> Kinetic parameters reported are for hydrolysis of l-Cth. Reaction conditions: 2 mM DTNB, 0.01–6.4 mM l-Cth and 0.068–6.6  $\mu$ M wild-type or eCBL variant, depending on the activity of the enzyme, in assay buffer at 25 °C. The data were fit to the Michaelis–Menten equation to obtain  $k_{cat}$  and  $K_{m}^{l-Cth}$  and Eq. 1 to obtain  $k_{cat}$  and  $K_{m}^{l-Cth}$ .

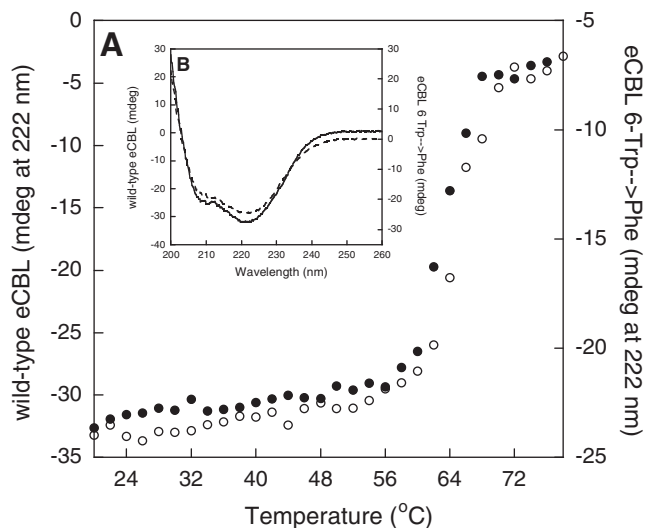


**Fig. 3.** Circular dichroism (A) thermal denaturation profiles at 222 nm and (B) spectra of 5.6  $\mu\text{M}$  wild-type eCBL (●, solid line) and the hextuple Trp  $\rightarrow$  Phe (○, dashed line).

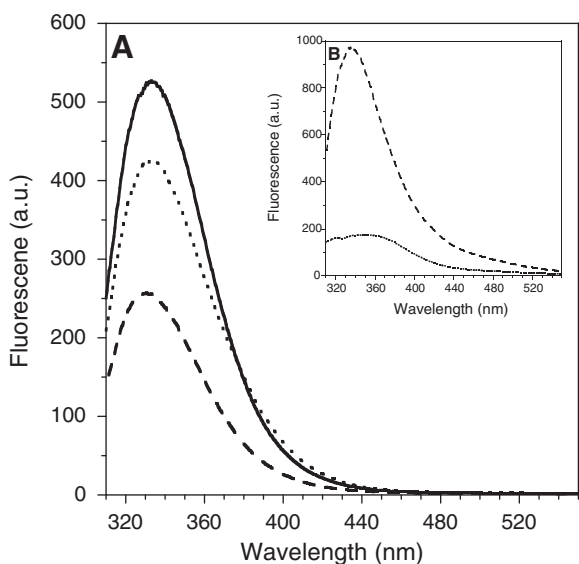


**Fig. 4.** Fluorescence spectra ( $\lambda_{\text{ex}} = 295 \text{ nm}$ ) of 20  $\mu\text{M}$  (A) wild-type eCBL (solid line), W230F (dashed line) and W340F (dotted line) and (B) the pentuple Trp  $\rightarrow$  Phe variants retaining W230 (pXW230, dashed line) and W340 (pXW340, dotted line).

decreases and red-shifts between 3 and 5 M and above 5 M urea (Fig. 5A and B). The emission maximum is shifted to 345 and 360 nm at 4 and 8 M urea, respectively (Fig. 5B and C). Comparison of the denaturation profiles of the 12 single and pentuple Trp  $\rightarrow$  Phe variants identified W188 as the residue that is released from quenching between 0 and 2 M urea as its replacement (W188F) results in elimination of the hyperfluorescent species, which is present in only one (pXW188) of the six pentuple Trp  $\rightarrow$  Phe variants (Fig. 5A). Variants that lack W340 and possess W188 (e.g. pXW188, tX + W340F and W340F) undergo a unique shift in fluorescence maxima to 380 nm upon incubation with 0.3–1.4 M urea (Figs. 5B and D and 6A). The 380 nm species results from fluorescence resonance energy transfer (FRET) between W188 and the enolamine tautomer of the internal aldimine of the PLP cofactor, in Schiff base linkage with K210, as demonstrated

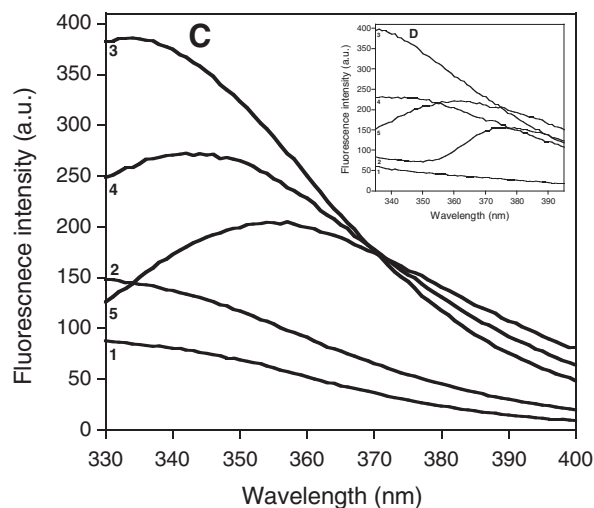
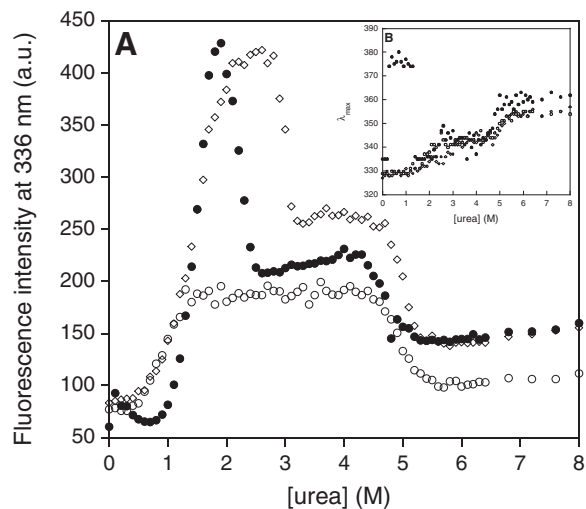


**Fig. 5.** The fluorescence (A) intensity at 336 nm and (B)  $\lambda_{\text{max}}$  of the urea denaturation profiles of 1  $\mu\text{M}$  wild-type eCBL (open diamond), W188F (open circle) and pXW188 (closed circle) and the corresponding fluorescence spectra of (C) wild-type eCBL and (D) pXW188 at (1) 0, (2) 1, (3) 2, (4) 4 and (5) 8 M urea.

by similar 380 nm peaks observed upon excitation of the tX + W340F and pXW188 variants at 295 (Fig. 6A) and 330 nm (Fig. 6B) [11]. The sharp decrease in fluorescence intensity between 3 and 3.5 M urea is likely due to aggregation, as centrifugation of samples prior to collection of spectra results in a decrease in the emission intensity in this range of urea concentration (Fig. 7). The circular dichroism spectrum of eCBL is dominated by the 208 and 222 nm minima characteristic of  $\alpha$ -helices (Fig. 2) and the increase in 222 nm absorption between 5 and 6 M urea suggests that secondary structure is maintained between 0 and 5 M urea (Fig. 7). The wild-type enzyme (30  $\mu\text{M}$ ) was incubated for 26 h with 1.4, 2.5, 3, 5 and 8 M urea prior to dilution to a final enzyme concentration of 1  $\mu\text{M}$  in 20 mM phosphate buffer, pH 7.5, to assess the ability of eCBL to refold. The presence of 2 M urea reduces eCBL activity by 95%. Recovery of 93%, 95% and 82% activity was observed following dilution of enzyme incubated in 1.4, 2.5 and 3 M urea, respectively. In contrast, dilution of enzyme incubated in 5 and 8 M urea results in the recovery of only 0.5% and 4% of activity, respectively, thereby providing support for proposed aggregation of the enzyme between 3 and 3.5 M urea and precluding thermodynamic analysis.

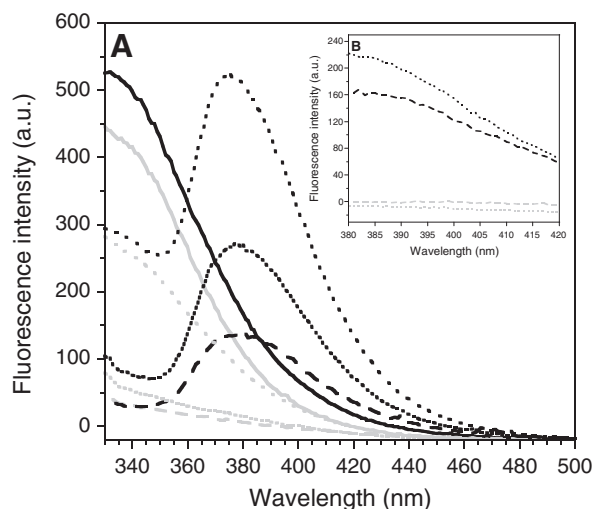


**Fig. 6.** Effect of 1.2 M urea on the fluorescence spectrum of 1  $\mu$ M wild-type eCBL (solid line), the pentuple Trp  $\rightarrow$  Phe variant pXW188 (dashed line), which maintains only W188, W340F (sparse-dotted line), and quadruple Trp  $\rightarrow$  Phe variant tX + W340F (close-dotted line), which maintains only W188 and W300. Fluorescence spectra for excitation at (A) 295 nm and (B) 330 nm were recorded in the absence of urea (gray lines) and in the presence of 1.2 M urea (black lines).

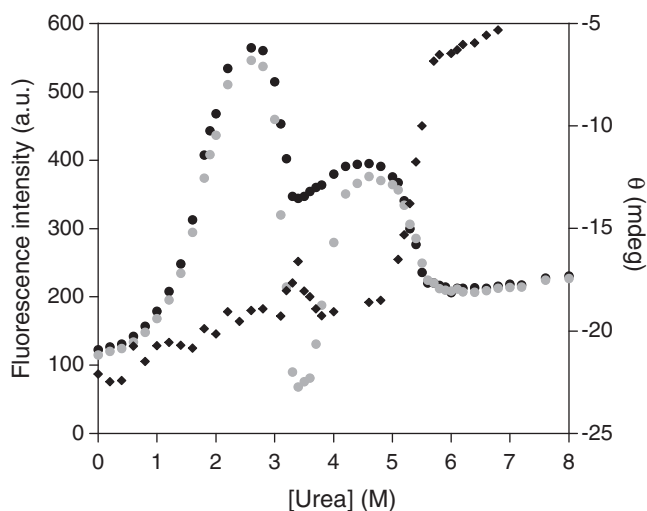


**Fig. 7.** Urea denaturation profiles of 5.6  $\mu$ M wild-type eCBL monitored via fluorescence ( $\lambda_{\text{ex}} = 295$  nm,  $\lambda_{\text{em}} = 338$  nm), prior to (black closed circle) and after (grey closed circle) centrifugation at 13500 rpm for 15 min, and circular dichroism spectroscopy at 222 nm (closed diamond).

## Discussion

The enzymes of the  $\gamma$ -subfamily of fold-type I provide a useful model system for investigations of the structure–function relationships underlying substrate and reaction specificity in PLP-dependent enzymes as their strong structural similarity extends beyond a common overall fold to the conservation of several key active-site residues [4,6,12]. The role(s) of the conserved active-site residues, shared by eCBL and eCGS, are influenced by the context of the specific active site [5,7,8]. However, the underlying features acting as determinants of specificity, including active-site dynamics and conformational changes, are not readily apparent from comparison of the available structures. Therefore, exploration of the complex and subtle nature of the determinants of reaction specificity among the enzymes of the  $\gamma$ -subfamily will be assisted by the development of conformational probes. The eCBL enzyme

provides an effective system for studies probing reaction specificity as structures of inhibitor complexes are available and the roles of 15 active-site residues have been characterized [2,5,7,13,14]. This study aims to provide tools to probe protein conformational changes in order to facilitate mechanistic and protein engineering studies of eCBL and related enzymes of the  $\gamma$ -subfamily.

Fluorescence and fluorescence quenching are effective methods to detect changes in protein conformation. In the case of proteins containing multiple tryptophan residues, characterization of each is necessary to access their efficacy as probes [15,16]. This is illustrated by studies employing site-directed mutagenesis to investigate the individual tryptophan residues of *Salmonella typhimurium* O-acetylserine sulfhydrylase (sOASS) and human  $\gamma$ D-crystallin [17,18]. However, the conservation of tryptophan in protein sequences is high and its substitution is commonly associated with reduced stability [17]. The six tryptophan residues of eCBL are common to  $\gamma$ -proteobacterial CBL sequences. In contrast, conservation at the corresponding positions is not observed for the closely related enzymes of the  $\gamma$ -subfamily, which suggests the feasibility of their conservative replacement with phenylalanine for the purpose of characterizing the contribution of each to the fluorescence spectrum of eCBL and to assess their ability to serve as conformational probes. The location of eCBL-W188 and W340 at the core and on opposite sides of the interface between the catalytic and carboxy-terminal domains, which form the active-site cleft, is well-suited to this purpose. Similarly, Campanini and coworkers characterized the tyrosine-substitution variants of the two tryptophan residues (W50 and W161) of sOASS, which are situated such that they provide sensitive probes of conformational changes in the amino and carboxy-terminal domains of this enzyme [17].

With the exception of the 8-fold increase in  $K_m^{\text{L-Cth}}$  of W340F, the effect of substituting the six tryptophan residues with phenylalanine on the kinetic parameters of eCBL is minor [7]. The  $k_{\text{cat}}$  and  $K_m^{\text{L-Cth}}$  of the W131F, W188F, W230F, W276F and W300F variants are within 1.6-fold and the catalytic efficiency of eCBL-pXW340, which possesses only W340, is reduced by 2.2-fold, compared to the wild-type enzyme (Table 1). Similarly, the minor differences between the CD spectra of the Trp  $\rightarrow$  Phe variants and the wild-type enzyme likely reflect the absorption of tryptophan in the far-UV region rather than changes in secondary structure (Figs. 2 and 3) [17,19]. The fluorescence spectra of the pentuple Trp  $\rightarrow$  Phe replacement variants were compared with the corresponding difference spectra, produced by subtraction of the spectrum of the remaining five tryptophan residues) from that of the wild-type enzyme. The spectrum of pXW340 is broadened and red shifted compared to the corresponding difference spectrum, suggesting a minor conformational perturbation that is localized to the interface between the two major domains and likely indicates a shift in the equilibrium between the open and closed conformations of the active site. Loss of  $\alpha$ -helical secondary structure, monitored by circular dichroism, resulting from thermal denaturation was employed to determine the relative effects of replacing the six tryptophan residues of eCBL with phenylalanine. With the exception of the 4.7  $^{\circ}\text{C}$  decrease in  $T_m$  observed for W188F, the effect of the individual Trp  $\rightarrow$  Phe substitutions on the thermostability of eCBL is minor. Replacement of W131, W230 and W300 with phenylalanine results in slight stabilization of the enzyme as the  $T_m$  of these variants is increased by 1.2–1.7  $^{\circ}\text{C}$  (Table 1). The observed additivity of the Trp  $\rightarrow$  Phe substitutions on thermostability is demonstrated by the 6.1 and 1.7  $^{\circ}\text{C}$  increases in  $T_m$  values, compared to the wild-type enzyme, of the pXW188 and hX proteins, respectively, which differ only in the presence of W188 in the former (Table 1, Figs. 2 and 3). In contrast with the common trend for correlation between increased stability and decreased activity, resulting from the

corresponding reduction in enzyme flexibility, no change in activity is observed for variants with increased thermostability, compared to the wild-type enzyme (Table 1) [18,20,21]. Thermodynamic parameters could not be calculated for eCBL because its denaturation is not fully reversible. Only 0.5% and 4% activity is recovered following refolding from 5 and 8 M urea, respectively.

The fluorescence spectrum of eCBL is dominated by W230 (Fig. 4). The feasibility of substituting this residue to reveal the fluorescence of residues better positioned to act as probes of active-site conformation is demonstrated by the negligible effects of W230F on the stability and kinetic parameters of eCBL. In contrast with W230, the contribution of W340 to the fluorescence spectrum is minor. Quenching of tryptophan fluorescence in PLP enzymes is common due to FRET between tryptophan and PLP or by direct interaction with the cofactor *via* short-range electrostatic interactions [15,22]. Quenching of W340 may reflect the latter process, given the hydrogen bond formed between the side chain of this residue and PLP-O3' and since FRET is not observed in the pXW340 variant, which possesses only W340 (Fig. 4). The minor contribution of W340 to the fluorescence spectrum of eCBL in combination with the observed 8-fold increase in  $K_m^{1-Cth}$  of W340F suggests that maintaining this residue, required for native activity, will not interfere with the use of other residue(s), such as W188, as conformational probe(s).

The residue responsible for the 5-fold increase in the 336 nm emission of eCBL between 0 and 2 M urea was identified as W188 by comparing the denaturation profile of the wild-type enzyme to those of the 12 single and pentuple Trp → Phe substitution variants (Fig. 5A). Similarly, a hyperfluorescent species corresponding to sOASS-W161 was reported, with maximum emission intensity between 0.8 and 1 M guanidinium hydrochloride, in the denaturation profile of the W50Y variant of sOASS [17]. The observed hyperfluorescence in eCBL may indicate a stable intermediate in the denaturation pathway or be due to release of quenching resulting from the reorientation of W188 caused by increased pre-transition flexibility of the native state [17]. The latter seems likely given the location of W188 at the interface of the two major structural domains that form the active-site cleft and the probability that movement of the domains relative to one another is required for catalysis. The sharp decrease in the emission intensity and redshift to 345 nm between 3 and 3.5 M urea (Fig. 5) in addition to the loss of fluorescence intensity in this range following centrifugation is indicative of aggregation (Fig. 7). This suggests that flexibility, particularly at the domain interface, is increased between 0 and 2 M urea followed by a conformational change between 3 and 3.5 M urea that exposes a hydrophobic surface, which results in the aggregation that precludes the refolding of eCBL.

The hyperfluorescence of W188 enables this residue, located in the active-site cleft, to act as a sensitive probe of subtle active-site conformational changes, as recently reported for chimeric variants of eCBL [23]. Comparison of eCGS and eCBL reveals two structurally distinct segments situated in proximity to the amino (region 1) and carboxy (region 2) termini, which are located at the entrance of the active-site. Analysis of 12 chimeric variants interchanging regions 1 and/or 2 of eCGS and eCBL demonstrated that exchange of region 2, in the context of eCBL, results in a ~3-fold increase in fluorescence emission at 336 nm, which is likely due to release of W188 from quenching, thereby reflecting a subtle alteration in the three-dimensional structure [23].

In wild-type eCBL, residue W188 is oriented such that it is quenched and FRET is not observed. However, the combination of the W340F substitution in the presence of 0.3–1.4 M urea, allows reorientation of W188 and/or PLP to permit FRET. Similarly, W177 of the  $\beta_2$  subunit of *E. coli* OASS was proposed to rotate relative to the cofactor, upon binding of the  $\alpha$  subunit, such that the

transition dipoles are no longer appropriately oriented with respect to one another to result in FRET [16]. Residues W188 and W340 of eCBL are bridged by L310, which contributes to the maintenance of their relative orientations [2]. Substitution of W340 may allow L310 to move, resulting in the reorientation of W188 with respect to the cofactor and enable the observed FRET, which demonstrates that maintenance of W340 is required for native active-site architecture. The release from quenching of W188 between 0 and 2 M urea and the observed FRET to the cofactor in the context of the W340F substitution in the presence of 0.3–1.4 M urea, demonstrate the sensitivity of W188 to changes in active-site architecture.

Substitution of W131, W230, W276 and W300 with phenylalanine, either individually or together (tX + W300F), does not affect the kinetic parameters, secondary structure or stability of eCBL (Table 1). This suggests that the quadruple Trp → Phe substitution variant tX + W300F can be employed as a model enzyme and raises the possibility of introducing other tryptophan residues in the context of the tX + W300F variant to directly probe other regions of interest. For example, substitution of a residue at the dimer interface (e.g. Y250 or Y343) with tryptophan would assist in identifying the region within the complex eCBL denaturation profile that corresponds to dissociation of the homotetramer to catalytic dimers since none of the six native tryptophan residues are located in proximity to the dimer interface.

The enzymes of the  $\gamma$ -subfamily of PLP-dependent enzymes demonstrate strong conservation in both structure and active-site residues. Recent studies have demonstrated that the roles of selected conserved active-site residues (e.g. eCBL-S339, which corresponds to eCGS-S326) depend on the context of the active site [5,8]. This demonstrates the subtlety of the features that act as determinants of specificity in this enzyme family and illustrates the necessity of developing tools to probe the complex structure–function relationships that underlie specificity. This study has identified the tX + W300F variant, in which residues W131, W230, W276 and W300 are replaced by phenylalanine, as a suitable model enzyme for mechanistic and protein engineering studies. The tX + W300F variant maintains wild-type kinetic parameters and stability while simplifying the fluorescence spectrum of eCBL, thereby enabling effective use of the sensitive probe of conformational changes at the active site and domain interface provided by the unique fluorescence properties of W188.

## Acknowledgment

The authors are very grateful to Drs. Joanne Turnbull, Judith Kornblatt, and Jack Kornblatt for their assistance with the circular dichroism experiments, suggestions for further experiments and interpretation of the eCBL denaturation pathway. This work was supported by the Natural Sciences and Engineering Research Council of Canada.

## References

- [1] J. Belfaiza, C. Parsot, A. Martel, C. Bouthier de la Tour, D. Margerita, G.N. Cohen, I. Saint Girons, Proc. Natl. Acad. Sci. USA 83 (1986) 867–871.
- [2] T. Clausen, R. Huber, R. Laber, H.D. Pohlenz, A. Messerschmidt, J. Mol. Biol. 262 (1996) 202–224.
- [3] T. Clausen, R. Huber, L. Prade, M.C. Wahl, A. Messerschmidt, EMBO J. 17 (1998) 6827–6838.
- [4] S.M. Aitken, P.H. Lodha, D.J.K. Morneau, Biochim. Biophys. Acta 1814 (2011) 1511–1517.
- [5] P.H. Lodha, S.M. Aitken, Biochemistry 50 (2011) 9876–9885.
- [6] A. Messerschmidt, M. Worbs, C. Steegborn, M.C. Wahl, R. Huber, B. Laber, T. Clausen, Biol. Chem. 384 (2003) 373–386.
- [7] P.H. Lodha, A.F. Jaworski, S.M. Aitken, Protein Sci. 19 (2010) 383–391.
- [8] A.F. Jaworski, P.H. Lodha, A.L. Manders, S.M. Aitken, Protein Sci. 21 (2012) 1662–1671.

- [9] A. Farsi, P.H. Lodha, J.E. Skanes, H. Los, N. Kalidindi, S.M. Aitken, *Biochem. Cell Biol.* 87 (2009) 445–457.
- [10] S.M. Aitken, J.F. Kirsch, *Biochemistry* 42 (2003) 571–578.
- [11] T.D. Turbeville, J. Zhang, G.A. Hunter, G.C. Ferreira, *Biochemistry* 46 (2007) 5972–5981.
- [12] S.M. Aitken, J.F. Kirsch, *Arch. Biochem. Biophys.* 433 (2005) 166–175.
- [13] T. Clausen, R. Huber, A. Messerschmidt, H.D. Pohlenz, B. Laber, *Biochemistry* 36 (1997) 12633–12643.
- [14] E.J. Ejim, J.E. Blanchard, K.P. Koteva, R. Sumerfield, N.H. Elowe, J.D. Chechetto, E.D. Brown, M.S. Junop, G.D. Wright, *J. Med. Chem.* 50 (2007) 755–764.
- [15] M. Arrio-Dupont, *Eur. J. Biochem.* 91 (1978) 369–378.
- [16] A.N. Lane, *Eur. J. Biochem.* 133 (1983) 531–538.
- [17] B. Campanini, S. Raboni, S. Vaccari, L. Zhang, P.F. Cook, T.L. Hazlett, A. Mozzarelli, S. Bettati, *J. Biol. Chem.* 39 (2003) 37511–37519.
- [18] J. Chen, S.L. Flaugh, P.R. Callis, J. King, *Biochemistry* 45 (2006) 11552–11563.
- [19] F.X. Schmid, in: T.E. Creighton (Ed.), *Protein Structure*, vol. 174, IRL Press, Oxford, 1997, pp. 261–297.
- [20] Z. Markovic-Housley, B. Stolz, R. Lanz, B. Erni, *Protein Sci.* 8 (1999) 1530–1535.
- [21] K.F. Fulton, S.E. Jackson, A.M. Buckle, *Biochemistry* 42 (2003) 2364–2372.
- [22] J.E. Churchich, *Biochemistry* 4 (1965) 1405–1410.
- [23] A.L. Manders, A.F. Jaworski, M. Ahmed, S.M. Aitken, *Biochim. Biophys. Acta* 1834 (2013) 1044–1053.